HIGH VELOCITY IMPACT ON TEXTILE REINFORCED COMPOSITES

Warnet L., Akkerman R., Ravensberg M.
University of Twente, Faculty of Engineering Technology, the Netherlands

Keywords: *Composite, 3D Textile, High Velocity Impact*

Abstract

Three types of fabric, 2D woven and 3D stitched, were compared on their impact performance. Tests were performed at three different rates, from quasi-static to high velocity impact (100m/s). The paper addresses the energy absorption capacity of these textiles. Visual observations of the damage as well as different types of instrumentation were used to evaluate the behavior of these textiles. Also the perforation energy was calculated or derived from the experimental data. At quasi-static conditions, the woven structure offers a better resistance to delamination, but a lower resistance to penetration. At higher velocities, the 3D textile having the highest stitch density gives the best energy absorption.

1 Introduction

Failure behavior of fiber reinforced plastics is a complex issue. Under impact conditions, multiple matrix cracking as well as fiber related fractures will occur under different stress situations. The damage development will depend, among other aspects, on the structure formed by the fibers, the impact velocity and the geometry considered.

A newly built gas-gun facility for High Velocity Impact (HVI) at the University of Twente gave the opportunity to compare the failure behavior of composite plates with that obtained with existing equipment during Low Velocity Impact (LVI) and Quasi-Static Impact (QSI). For this purpose, three Epoxy Vinylester glass fiber based composites with varying fiber structure (2-D and 3-D weaves, supplied by 3TEX) were analyzed for their failure behavior at different velocities. In all cases the plate geometry and the clamping conditions were kept constant.

The damage development was observed in detail during the quasi-static test. Results obtained during these tests were used as a basis for comparison for the higher velocities. The amount of damage that occurred in the different structures was analyzed for the used velocities. Also the energy absorbed by the different specimens was derived from the experiments. Conclusions are drawn on the impact behavior of the glass structures considered.

2 Experimental procedures

2.1 Material

Three types of E-glass based textiles were used to reinforce an elastomer modified Epoxy Vinylester resin (Dow Derakane 8084). Two 3D weaves were used, as well as a plane weave as a reference. The 3D weaves are built up from unidirectional layers stitched together with an E-glass yarn. 70 mm x 70 mm specimens were cut from plates produced with VARTM at 3TEX. Thickness varied depending on the structure between 4.7 mm and 5.7 mm. An overview of the important data concerning the three types of plates is given in Table 1.

2.2 Equipment

Three types of equipment were used to apply an impact loading to the specimen at High Velocity Impact (HIS) conditions, Low Velocity Impact (LVI) and Quasi Static Impact (QSI).

2.2.1 High Velocity Impact equipment

A gas gun was used for the highest velocity. This device is simply based on a 5 m long cylinder (diameter 38 mm) ending in the clamping system for impacting the specimens. The pressure was built up in the opposite part of the cylinder, separated from the rest by a thin polymer film. Puncture of this film releases a pressure wave, driving a purpose build indenter. The indenter was based on a 12.5 mm diameter cylinder with a spherical tup. The indenter was supported by two plastic disks, which

Table 1: Material data of the three tested types of textile.

Material	1		2		3	
ID	9-Layer 2D		2-layer 3D		1-Layer 3D	
Fabric type	Plain Weave		3D-weave		3D-weave	
Producer	Fibertech		3TEX		3TEX	
Type	-		P3W-GE001		P3W-GE012	
N° of layers	9		2 x 7 layers		1 x 7 layers	
Areal weight per layer [g/m^2]	800		3218		7207	
Fibre type	E glass roving					
Sizing	Polyester & vinylester compatible					
Resin type	Rubber-toughened epoxy vinyl ester					
Resin ID	Dow Derakane 8084					
Process	VARTM 96kPa					
Thickness t [mm] (STDEV)	5.74 (0.12)		4.72 (0.07)		5.41 (0.05)	
Areal weight [kg/m^2]	10.24		8.53		10.16	
Glass mass fraction [%]	68.2		71.7		70.8	
	Warp	Fill	warp	Fill	warp	Fill
Flexural Modulus [GPa]	20.1	15.3	-	21	-	23.4
Tensile Modulus [GPa]	22.9	22.3	31.2	26.5	26.2	25.7
Flexural Strength [MPa]	505	433	-	535	-	580
Tensile Strength [MPa]	390	319	456	418	441	494
Compressive Strength [MPa]	372	285	689	361	305	351

guaranteed the indenter would perform its impact in the center of the specimen. The front disk was made of a brittle PS, which was triggered to fracture just before it hits the specimen. The second at the back of the indenter was made of a tough PC, simply held longitudinally by a brittle washer. It is assumed that the fracture of the brittle material did not absorb any significant amount of energy. Mass of the complete indenter was 86 g.

The composite plate was clamped at the end of the pressure cylinder with a purpose built set-up. A drawing of the device with the indenter before and after impact can be found in Fig. 1.

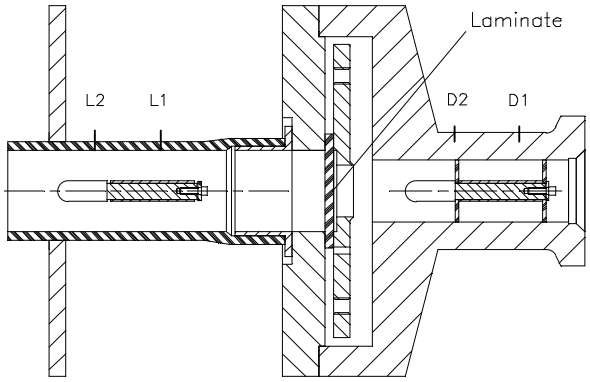

Fig. 1. Gas-gun set-up showing the indenter before (right) and after (left) impact. Velocities are measured using transducers located at D1 and D2, L1 and L2.

Its principle was taken over from a Dynatup impact machine clamping system. The specimen was clamped between two steel plates having a 50 mm diameter opening, held together by four pneumatic cylinders (not shown on Fig. 1).

The instrumentation of the High Velocity Impact test is limited to the measurement of the velocity of the indenter before an after the impact. The velocity before impact is measured with two piezoelectric pressure transducers mounted in the cylinder just before the specimen. Two photoelectric cells with lasers were used to measure the velocity after impact. A four channels oscilloscope was used to monitor the sensors and derive the velocities. With a 70MPa pressure, impact velocities V_{imp} varying from 100 m/s to 120 m/s were measured. The variation in impact velocity is due to the variation in pressure, as well as variation in the way the film releasing the pressure wave did fracture.

After impact, the remaining energy of the indenter was absorbed by a sand filled tube.

2.2.2 Low Velocity Impact equipment

A Dynatup 8250 Instrumented Falling Weight Impact Machine (IFWIM) was used for the low velocity impact tests. A 12.5 mm spherical indenter was fixed to a 35kN capacity Kistler piezoelectric loading washer. The clamping of the specimen was performed with a Dynatup pneumatic device, whose principle was used to design the clamping device of

the high velocity set-up. The mass and velocity were chosen to obtain a comparable kinetic energy level as with the high velocity set-up. A combination of an impact velocity V_{imp} of 9 m/s and a mass of 12 kg was chosen.

The instrumentation involved logging the force-time response with an oscilloscope. Double integration of this response resulted in a calculation of the displacement.

2.2.3 Quasi Static Impact equipment

An Instron servo hydraulic universal testing machine was used to perform the quasi static test. Most features used for the falling weight impact tests were also adopted here. This includes the indenter with Kistler load washer, as well as the clamping system. Displacement was measured using the in-situ LVDT of the tester. A velocity of 0.2mm/s was used. As extra instrumentation a CCD camera was placed under the clamping system. The translucent material used made it possible to monitor some aspects of the damage development during testing.

2.3 Experimental program

The experimental program focused in first instance on the tests at high velocity. Three specimens were tested per reinforcement types. At the low-velocity impact conditions, specimens were used to find the energy necessary to perforate the specimen. Tests at comparable impact energy as at high velocity were also performed. A few specimen were also reserved for characterizing the damage development quasi-statically.

3 Results

3.1 Damage development

3.1.1 Quasi static tests results

Due to its inherent low velocity, the quasi-static test provides most of the information required to analyze the different damage mechanisms involved. Fig. 2 shows the quasi-static force-displacement diagram of the 3D 1 layer specimen.

One can separate such force-displacement graphs in four sections as shown in Fig. 2. An illustration of the corresponding damage is given in the form of a selection of pictures taken from the underside of the translucent material in Fig. 3.

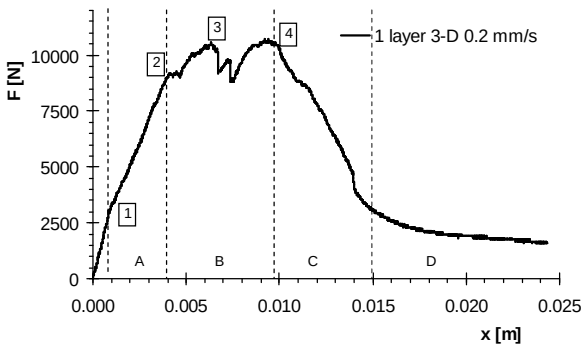

Fig. 2. Quasi static force-displacement of the 3D 1 layer specimen

- At the start of the test only a shadow from the indenter is visible. Until section 'A' starts, no damage at the macro scale can be observed. At x=2 mm (Pict. 1), the section 'A' starts, corresponding with a change in compliance in the force–displacement diagram. Physically, a few transverse cracks occur, followed by delaminations in different layers. The resulting picture after delamination growth is pict 2 in Fig. 2. It is worth noting at this point that in the case of the stitched material, the delamination can be qualified as bundle delamination. The area of such a delamination does not actually cover a circle or ellipse, but is roughly limited by the stitches to the bundle projected area width. In the 2 layers 3D material, the 'projected' picture given by the camera means their presence is overshadowed by a traditional interlaminar delamination, running between

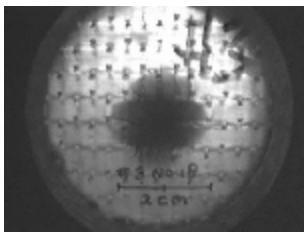
Pict. 1 (x = 2 mm)

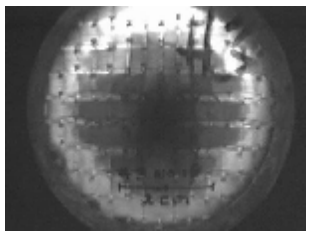
Pict. 2 (x = 4.1 mm)

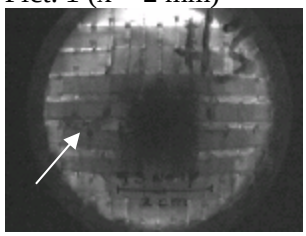
Pict. 3 (x = 6.5 mm)

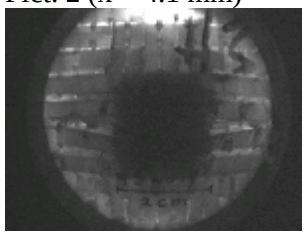
Pict. 4 (x = 9.2 mm)

Fig. 3. Picture taken during QS impact under the specimen.

the two stitched layers. For the woven material, traditional interlaminar delaminations occur between the different layers, but do not induce any reduction in compliance. These delaminations grow steadily with increasing force until section 'B' (pict. 2 at x=4.1mm). It is worth adding that the projected delamination surface of the woven reinforcement was smaller than that of the stitched systems. The delamination surface was also smaller than the clamping boundaries. However, most bundle delamination of the stitched structures did reach the edges of the clamping device. This is shown in Fig. 5, where the impact and bottom side of woven and 3D 2layers plates are photographed after testing.

- The start of section 'B' is characterized by a discontinuity in the force-displacement. It can be observed from the top side that penetration starts at this point, accompanied with fiber fracture. for the 3D structures, stitch fracture occurs in this section, shown at the arrow in the picture 3 at x=6.5 mm for the 3D material. Several mechanisms are induced by the penetration of the indenter. Bundles at the circumference of the spherical indenter are pushed aside, effectively fracturing the stitch. During penetration, most bundles of the stitched structures are fractured under shear, other near the free surface are pulled out or fractured. This illustrated in Fig. 4. For the woven textile, it seams that the fiber bundle are fractured under shear predominance.
- In the section 'C', force decreases. This corresponds with the last phase in the penetration of the spherical indenter. In the case of the woven structure, the picture of the bottom side in Fig. 5 shows that parts of the laminate near the free surface fail under bending (see also sketch).

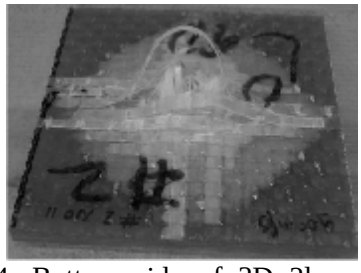

Fig. 4. Bottom side of 3D 2layer specimen after impact testing, illustrating bundle delamination and pull-out.

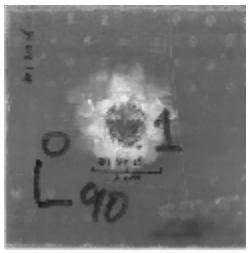

Woven top side

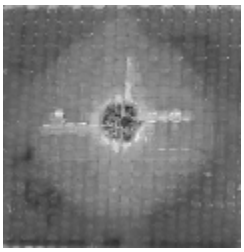

3D 2Layers top side

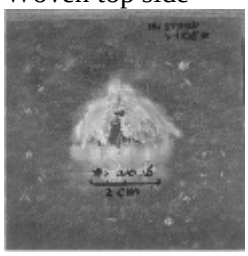

Woven bottom side

3D 2Layers bottom side

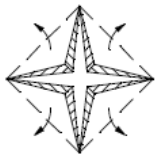

Fig. 5. Impact and bottom side of woven (left) and 3D 2layers plates.

- In Section 'D', only the friction of the indenter in the fractured material induces a residual force. After removing the indenter, no extreme permanent deformation was observed on the impact side.

The force-displacement diagrams of the three types of material in the same quasi static conditions are given in Fig. 6. The first difference between the three materials already shows up in the first part of the graph. Although the initial matrix cracking / bundle delamination in the 3D reinforcement leads to a clear increase in plate compliance, the woven plate does only show non-linearity at a higher load level, shortly before the maximum load is reached. The fact that bundle delamination occurs at a lower load indicates a lower mixed mode fracture toughness of the stitched bundles compared to the mixed mode interlaminar fracture toughness of the woven structure. As the matrix material is identical for the three types of plate tested, this can be attributed to the woven clothe intrinsic waviness, compared to the basically unidirectional 3D structure. Also the projected delamination area is significantly lower for the woven textile than for the 3D structures.

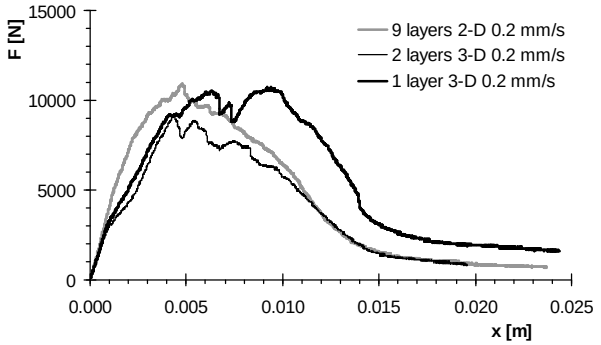

Fig. 6. Quasi static force-displacement diagrams of the three materials

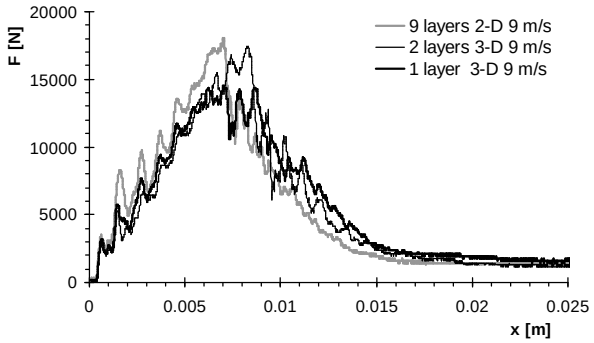

Fig. 7. Low velocity impact force-displacement diagrams of the three materials

Further differences between the three materials are found in the period after the maximum load is reached. The force-displacement graph of the single layer 3D material clearly shows that more energy is absorbed by the stitched structure. The value of the absorbed energy at perforation (until section 'D'), is evaluated at a displacement of 15 mm for all three systems. The absorbed energy at perforation E_{perf} reached 113 J for 1 layer 3D structure, 80 J for the 2 layer 3D plates, 96 J for the woven textile. The relatively low energy absorption of the 3D 2 layers system is partly due to the lower thickness of the plates tested. At equivalent thickness, the 1 layer 3D specimens behave significantly better than the woven version.

3.1.2 Low Velocity Impact tests results

Falling weight impact tests were performed with a 12kg mass at an impact velocity of 9 m/s, corresponding to a kinetic energy E_k of 486J. Typical force-displacement diagrams for the three different materials are shown in Fig. 7.

The maximum force reached in these tests is significantly higher than during the quasi static tests. Although significant differences in the shape of the quasi-static response were observed between the three types of structures, no such conclusion can be drawn for the responses at 9m/s. The better energy absorbing capacity of the 3D stitched textiles does not seam to be revealed in these conditions.

The major difference between the observed damage after impact and quasi static testing was the projected delamination surface. It covered the full free surface of the specimens for the three types of material.

It is remarkable that calculating the energy absorbed by the system at perforation (evaluated at 15mm deflection) leads to similar values of 118 J, 119 J and 122 J for the 2D woven, 3D single layer and 3D 2 layers respectively. Still one should be careful in drawing any conclusions, as the thickness of the 2 layers 3D material was lower than that of the two others types of reinforcement.

The velocity at which the indenter just perforated the specimen was also measured. It varied from 4.5 m/s (E_k=120 J) for the woven structure, to 4.3 m/s (E_k=110 J) for the 3D 2 layers textile, and 4.7 m/s (E_k=130 J) for the 1 layer system. The corresponding energies compare well to the energy at perforation evaluated for the excess energy test at 9m/s mentioned above.

3.1.3 High Velocity Impact test results

As explained earlier, the only results obtained through the high velocity test set-up were the velocity before V_{imp} and after impact V_{res}. Table 2 lists these velocities for 3 specimens of each type of textiles. Also the kinetic energy E_k and the absorbed energy E_{abs} are evaluated.

Table 2: Velocity before and after impact, kinetic and absorbed energy.

Test	V_{imp} [m/s]	V_{res} [m/s]	E_k [J]	E_{abs} [J]
2D-9L-1	115	83	572	293
2D-9L-2	108	70	505	305
2D-9L-3	124	88	659	350
3D-2L-1	111	72	537	322
3D-2L-2	100	61	433	281
3D-2L-3	114	72	562	351
3D-1L-1	120	87	623	315
3D-1L-2	104	68	468	280
3D-1L-3	124	87	665	357

As explained earlier, the variation in impact velocity is due to the variation in gas pressure, as well as in the way the film releasing the pressure wave is punctured. The absorbed energy E_{abs} is calculated by subtracting the rest kinetic energy E_{res} of the indenter after puncture from the impact energy E_k:

$$E_{abs} = E_k - E_{res} \quad (1)$$

The values quoted in Table 2 can not be straightforwardly compared to the absorbed energies mentioned earlier for the QS and LVI tests. In the high velocity tests, a significant amount of energy is also absorbed by friction of the indenter (85 mm long) in the composite plate just after penetration. An attempt to compare the influence of the three velocity levels on the energy partitioning will be discussed in the next section.

The results show as well that it would have been more satisfying to test more than three specimens per type of textile. The scatter in absorbed energy is relatively large within one type of textile.

Visually, the specimens show an increased projected delamination area compared to the one tested at low velocity. Damage is also present in the clamping, showing the limitation of the system. Interesting as well is the permanent deformation on the impact side observed for the 3D stitched specimens, especially for the single layer specimens

3.2 Energy at perforation

A common way of analyzing the results from high velocity impact is to perform an energy partitioning analysis [[2,[3]. The absorbed energy is partitioned in terms representing different failure mechanisms. Mines et al [[3] identified for example the energy absorption mechanisms as delamination, shear induced perforation and friction terms. Evaluating these terms often necessitate the knowledge of material behavior / properties. For the energy level involved in the occurrence of delamination for example, knowledge of the delamination fracture toughness of the system under mixed mode is required. Difficulties are found to control dynamic effects in these difficult to interpret tests. A review by Jacob [[1] shows a lack of consensus about the effect of loading rate on the fracture toughness properties in composite materials. The general impression is that fracture toughness will decrease with rate and in some cases show rate invariance. This does agree qualitatively with the observed increase in delamination area with load rate in this paper.

As no relevant material data is available at this moment for the materials tested, no quantitative partition analysis was performed at this stage. It is still informative to consider the energy absorbed at the moment the specimen is just perforated E_{perf}. Referring back to the different sections defined in Fig. 2, this is the energy obtained by integrating the force-displacement data until section 'D'. It is assumed that the energy component in section 'D' is only due to friction of the indenter in the perforated specimen. Integrating the force-displacement response in this period gives an average friction energy E_f. Dividing this energy by the displacement gives an average friction energy per unit length $E_{f/L}$. These values can be calculated for both the quasi-static as the low-velocity conditions. It is chosen to use the value measured at low-velocity impact to evaluate the energy absorbed by friction during the high velocity tests. The energy absorbed at perforation E_{perf} by the specimen (and actually the set-up as a whole) at high velocity is then obtained from:

$$E_{perf} = E_{abs} - E_{f/L} \times L \quad (2)$$

Where E_k is the kinetic energy, E_{abs} the total absorbed energy as derived from the velocity measured after impact, $E_{f/L}$ the friction energy by unit length and L the length of the indenter.

Table 3 summarizes these values for the three structures and the three test rates. The results of the perforation energy clearly show for all three structures an increase in energy absorbing capacity with the test rate. The significant difference in thickness between the different structures makes it difficult to compare the performance of the type of structure. A study by Gellert et al [[4] suggested a bilinear relation between thickness and perforation energy for a large series of test performed on woven glass reinforced vinylester. Their measurement covered a wide range of thicknesses. Assuming this assumption is also valid for the test presented here, the relatively narrow range of thicknesses would mean a linear relation between thickness and perforation energy. The perforation energy relative to the specimen thickness is shown in the last column of Table 3, as well as in Fig. 8. Under quasi static conditions, comparing the perforation energy gives similar results for the woven and the 3D 2layers structures. As shown earlier in Fig. 6, the 3D 1layer textile is better at absorbing energy.

Table 3: 'Macro' Energy components for the different rate conditions

Material	*Thick.* [mm]	V_{imp} [m/s]	V_{res} [m/s]	E_c [J]	E_{abs} [J]	$E_{f/L}$ [J/mm]	E_{perf} [J]	E_{perf} [J/mm]
2D-9L	5.74	0.0002		-		1.1	96	16.7
		9		486		1.5	118	20.6
		116	83	580	315	1.5	188	32.8
3D-2L	4.72	0.0002		-		1.1	80	16.9
		9		486		1.7	119	25.2
		108	72	509	318	1.7	174	36.8
3D-1L	5.41	0.0002		-		2.2	114	21.1
		9		486		1.9	122	22.6
		116	87	585	317	1.9	156	28.8

Under impact conditions however, the 2 layers stitched material performs significantly better. Although it is difficult to quantify, the 3D 1 layer material showed more damage after both impact tests. Also the permanent deformation after high velocity impact was particularly large for this structure. Why the 2 layers perform better than the single layer under these conditions is difficult to answer. A possible explanation lies in the difference in bundle size. Although not quantified, the 2 layer system offers a finer structure, effectively having more stitches.

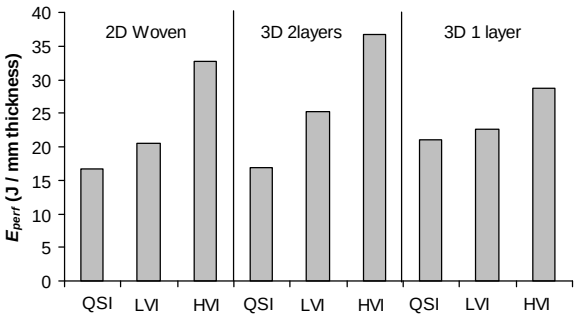

Fig. 8. Perforation energy relative to the specimen thickness for the three types of structures and the impact rate

4. Conclusions

A traditional woven fabric reinforced plastic and two stitched 3D structures were compared on their impact performance. Tests were performed at three different rates, from quasi-static to high velocity impact (100m/s). Different types of instrumentation were used to support the observations on damage development. Also the perforation energy was calculated or derived from the experimental data.

At quasi-static conditions, the woven structure offers a better resistance to delamination, but a lower resistance to penetration. At higher velocities, the 3D textile having the highest stitch density gives the best energy absorption. The energy at perforation helps quantifying the energy absorption capacities of the testing glass structures. Still, this 'macro' energy does not provide any relation to the occurring damage. A thorough model meant to quantify the energy absorbed by the different damage mechanisms is still necessary for this type of study.

References

[1] Jacob G.C., Starbuck J.M., Fellers J.F, Simunovic S., Boeman R.G. "The effects of loading rate on the fracture toughness of fibre reinforced polymer composites". *J. of Applied Polymer Science*, Vol. 96, pp 899-904, 2005.

[2] Zee R.H., Hsieh C.Y., "Energy loss partitioning during ballistic impact of polymer composites". *Polymer Composites*, Vol. 14, pp 265-271, 1993.

[3] Mines R.A.W., Roach A.M., Jones, N. "High velocity perforation behaviour of polymer composite laminates". *International Journal of Impact Engineering*, Vol. 22, pp 561-588, 1999.

[4] Gellert E.P., Cimpoeru S.J., Woodward R.L. "A study of the effect of target thickness on the ballistic perforation of glass-reinforced plastic composites". *International Journal of impact engineering*, Vol 24, pp 445-456, 2000.